Construction and Building Materials 287 (2021) 123021

Contents lists available at ScienceDirect

Construction and Building Materials

journal homepage: www.elsevier.com/locate/conbuildmat

Improvement on rheological property of asphalt binder using synthesized micro-encapsulation phase change material

Tam Minh Phan, Dae-Wook Park *, Tri Ho Minh Le

Dept. of Civil Engineering, Kunsan National University, Gunsan-si 54150, Jeollabuk-do, Republic of Korea

HIGHLIGHTS

- Two μPCMs were successfully synthesized via encapsulation method.
- $CaCO_3$-μPCM presented good thermal stability with 95% residual weight at 160 °C.
- SiO_2-μPCM acquired prime encapsulation ratio (R_E = 52.9%).
- μPCMs released latent heat that increased asphalt binder temperature of 1.5 °C.
- Both μPCMs enhanced thermal cracking resistance by reducing binder stiffness.

ARTICLE INFO

Article history:
Received 20 January 2021
Received in revised form 26 February 2021
Accepted 8 March 2021
Available online 25 March 2021

Keywords:
Asphalt binder
Synthesized PCMs
Rheological property
Thermal cracking
Black ice

ABSTRACT

Temperature is a governing parameter that affects the rheological property of asphalt binder. Upon cooling, bitumen becomes stiffer and prone to thermal cracking. To reduce the negative impact of temperature, utilizing the thermal energy storage of phase change material is a promising solution. This study provides an approach to synthesize micro-encapsulation phase change material (μPCM) and its application to enhance the binder's rheological property and mitigate black ice. Two μPCMs were prepared with n-Tetradecane as a core, while Calcium carbonate ($CaCO_3$) and Silicate (SiO_2) as a shell. SEM test exhibited that μPCM had a spherical shape with a diameter ranging from 1 to 7 μm. Meanwhile, thermogravimetric analysis proved that the encapsulation method could protect and prevent leakage of n-Tetradecane under high temperature. The residual weight of $CaCO_3$-μPCM was 95% and 84% at 160 °C and 350 °C, respectively. The differential scanning calorimeter results showed that the encapsulation ratio was approximately 52.9% (ΔH = 99.94 W/g). Moreover, different μPCM modified asphalt binders were examined to evaluate the rheological property. Results from rotational viscosity test at 135 °C pointed out that adding μPCM did not affect binder viscosity. DSR test showed that the incorporation of μPCM could reduce binder stiffness at low temperatures. The thermal effect of μPCM was analyzed by low-temperature sweep test. With simultaneous cooling, μPCM released latent heat, thus increasing the binder's temperature by 1.5 °C. The low values of $G^*\sin\delta$ indicated the outperformance of μPCM-binder compared to conventional binder in terms of thermal cracking resistance.

1. Introduction

Asphalt mixtures are widely used to pave roads and highways due to their advantages, such as safety, smoothness, and construction time. During its service life, asphalt road surfaces are directly exposed to environmental conditions [1]. Other than traffic load, asphalt pavement must withstand seasonal and diurnal variations in temperature [2]. Several studies pointed out that environmental factors, especially ambient temperature, impose significantly impact on the asphalt pavement [3–5]. Temperature change influences internal pavement stress and strain, its deformation, and thermal cracking. Nowadays, to improve the performance of asphalt pavement, and extending its service life is challenging for researchers. The conventional improvement of pavement can exhaust the use of natural resources. Many studies have been developed to reduce the burden on natural resources by utilizing by-products [6,7]. Some include using fibers to enhance the performance [8,9], and others utilize self-healing material to extend service life [10,11]. Moreover, the enhancement on the binder's rheological property using varied modifiers is a key tool to improve the overall asphalt mixture performance. Asphalt binder plays an

* Corresponding author.
E-mail address: dpark@kunsan.ac.kr (D.-W. Park).

https://doi.org/10.1016/j.conbuildmat.2021.123021
0950-0618/

essential role in an asphalt pavement system [1]. During low temperatures, asphalt binder can become stiff reaching a brittle condition resulting to thermal cracking. Thus, repeating the freeze and thaw process is one of the primary pavement distresses. In the winter season, snow and ice can reduce the friction between the tire and road surface. This is especially dangerous during black ice formation. The black ice phenomenon is hazardous on driving and affects the temperature cracking of asphalt pavement. Several methods have been developed to mitigate the adverse effects of low temperature such as road salt, using a gas-fired or electric boiler, and incorporating phase change material [11–13].

Phase change material (PCM) is a latent heat fusion material that releases/absorbs latent heat during the melting/crystallization process [14]. At the melting temperature (solid–liquid transition), PCM absorbs thermal energy. Then, the stored thermal energy will be released when the surrounding temperature is lower. PCM has been receiving attention in various applications. Several studies have been incorporating PCM in asphalt mixture to moderate pavement temperature. For instance, the appropriate dosage of PCM could regulate extreme temperature and reduce rutting of asphalt pavement [15,16]. Besides, PCM was also used to delay or prevent pavement freezing at a low temperature. The research done by Manning et al. proved that containing of PCM-6 (6 °C phase change) could mitigate the impact of frozen process freezing [12]. Karka et al. showed that PCM has a vital ability on thermal regulation of asphalt mixture [13]. It is well known that the phase change temperature is a critical factor that tightly associates with the warming or cooling temperature of asphalt mixture. The effect of phase change material on thermal properties of asphalt pavement has been calculated by the Finite Element Model (FEM) [17].

Nevertheless, direct incorporating PCM into asphalt mixture is restricted due to leakage and weak thermal stability [14]. The leakage caused a reduction in adhesion between aggregate and asphalt binder, resulting in lower asphalt mixture's performance. Therefore, different ways have been developed to mitigate the leakage problem and enhance thermal stability. Wang et al. provided a novel microencapsulated PCM with $CaCO_3$-shell and paraffin-core [18]. Fang et al. recommended the micro-encapsulation process using silicate (SiO_2) as a shell and n-Tetradecane as a core [19]. Both encapsulated PCMs presented a high storage latent heat and good thermal stability. Nowadays, many studies have been developed to enhance the rheological property of asphalt binders at low temperatures, such as utilizing bio-oil [20], using SBS (styrene–butadienestyrene) modified asphalt binder [21], and incorporation of PCM in asphalt binder [22]. Due to the releasing latent heat, PCM was utilized to improve the rheological property of asphalt binder at low temperature.

In this research, to improve the rheological property of asphalt binder and mitigate black ice phenomenon at low temperature, a one-dimensional (1D) numerical model of PCM modified asphalt pavement was developed to calculate the optimal phase change material (such as PCM's content, phase change temperature, latent heat fusion). Based on the FEM results, two micro-encapsulation phase change materials were synthesized using the encapsulation method. Two shell-materials were developed, including Calcium carbonate ($CaCO_3$) and silicate (SiO_2). Serval laboratory tests was then conducted to examine the properties of μPCMs. A scanning electron microscope (SEM) was employed to observe the morphology, diameter, and surface of μPCM. While a thermogravimetric analysis was adopted to specify the thermal stability. Differential scanning calorimeter (DSC) determined the phase change properties such as phase-change temperatures and latent heat fusion. Subsequently, base asphalt binder (PG 64–22) was modified with the two new μPCMs to investigate the effect on rheological property. This investigation included rotational viscosity test (RV), dynamic shear rheometer test (DSR), and low-temperature sweep test. The whole process can be referenced in Fig. 1.

2. Design and preparation of micro-encapsulation phase change material

2.1. Optimum phase change material design

The one-dimensional (1D) heat transfer has been widely used to predict pavement surface temperature. This is because the pavement thickness is smaller than other dimensions of the road [4]. The governing equation of heat transfer is written in Eq. (1). Where, ρ = density (kg/m^3); c_ρ = specific heat capacity; T = temperature (°C) t = time (s); z = thickness (m).

$$\rho c_p \frac{\partial T}{\partial t} = \frac{\partial}{\partial z}\left(k \frac{\partial T}{\partial z}\right) \tag{1}$$

Asphalt concrete's thermophysical properties are related to aggregate types, air voids, and mineral particles [5,23]. Besides, pavement temperature also depends on the effect of external factors as shown in Fig. 2. For example, the pavement surface is affected by solar radiation, air temperature, wind speed, and convection between the surface and surrounding air [17]. Equation (2) shows the total boundary heat flux (Q) at the surface temperature involved in the heat exchange with the surrounding. The absorbed heat flux (q_r) is highly dependent on the thermal absorptivity of asphalt pavement and incident solar radiation [4,24]. The longwave length heat flux (q_l) is related to the sky's fraction covered by the clouds [25]. While Hermansson's research presented the convection heat flux (q_c) between asphalt pavement and the surrounding air [3]. Moreover, the asphalt pavement emits infrared thermal radiation to the surrounding as a function of temperature. Report indicates that the emissivity of asphalt pavement usually ranges from 0.80 to 0.93 [4].

$$Q = q_r + q_l - q_c - q_e \tag{2}$$

Several studies have considered the effect of incorporating PCM in asphalt concrete to improve the volumetric heat capacity (ρc_{peff}) as shown in Eq. (3) [17,26]. Where, ϕ = PCM volume (%); ξ = the volume fraction of PCM (%); ρ_{AC} = asphalt concrete density (kg/m^3); ρ_{PCM} = PCM density (kg/m^3); $c_{\rho s}$, $c_{\rho l}$ = specific heat capacity of PCM (J/kgK); $c_{\rho AC}$ = specific heat capacity of asphalt concrete (J/kgK).

$$\rho c_{p_{eff}} = \phi \rho_{PCM}(\xi c_{p_l} + (1-\xi)c_{ps}) + (1-\phi)\rho_{AC}c_{p_{AC}} \tag{3}$$

Besides, the thermal conductivity of PCM-modified asphalt concrete is related to the matrix's thermal conductivity. This value can be expressed by PCM's volume fraction, and thermal conductivity of asphalt concrete and PCM. Karol and Tomasz recommended that the effective thermal conductivity can be calculated by the Maxwell model [26]. The expression can be referenced from Eq. (4). Where, k_{eff} = effective thermal conductivity (W/mK); ϕ = PCM's volume (%); k_{AC}, k_{PCM} = thermal conductivity (W/mK) of AC and PCM, respectively.

$$\frac{k_{eff}}{k_{AC}} = 1 + \frac{3\phi}{\left(\frac{k_{PCM}+2k_{AC}}{k_{PCM}-k_{AC}}\right) - \phi} \tag{4}$$

Based on the Maxwell model, the thermal conductivity of PCM was calculated only if PCM content was lower than 25% of total mixture volume. The k_{PCM} was depended on the liquid and solid fractions, as shown in Eq. (5). Where, ξ = volume fraction (%); k_l, k_s = thermal conductivity (W/mK) at liquid and solid phase, respectively.

$$k_{PCM} = \xi k_l + (1-\xi)k_s \tag{5}$$

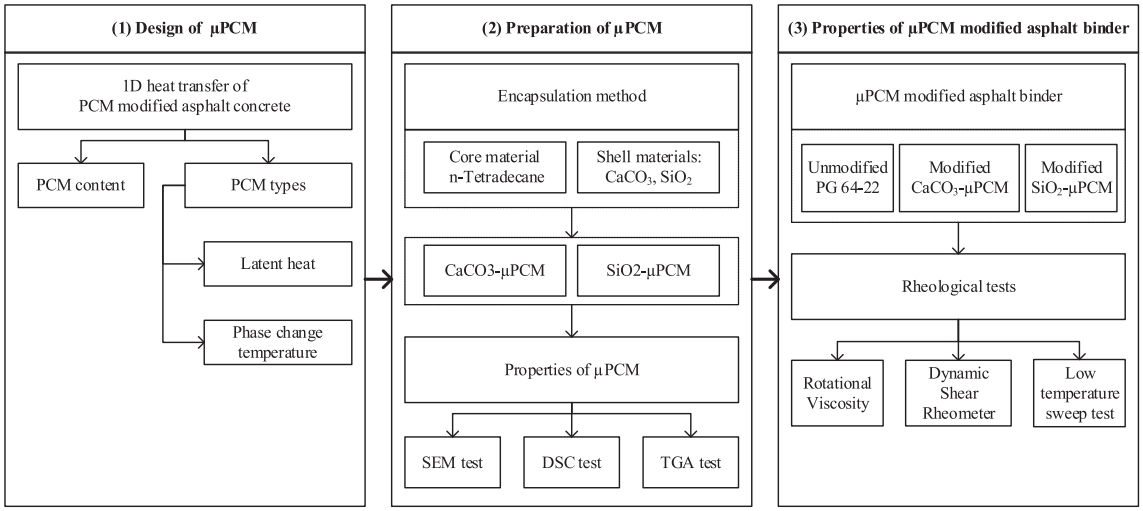

Fig. 1. Research flowchart.

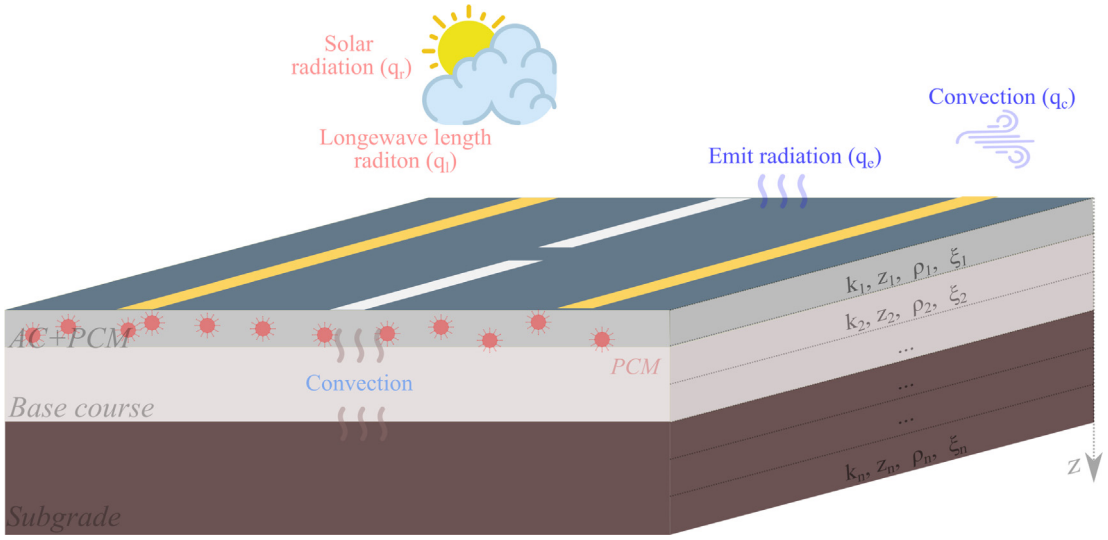

Fig. 2. Pavement temperature profile.

Report suggests that the PCM's volume fraction has a tight correlation with the temperature [17]. The expression of volume fraction is written in Eq. (6). Where, ξ(T) = volume fraction at the temperature T (%); T = temperature (°C); T_l, T_s = liquid and solid temperature (°C), respectively.

$$\xi(T) = \begin{cases} 0, & T < T_s, \quad Solid\ phase \\ \frac{T-T_s}{T_l-T_s}, & T_s < T < T_l, \quad Mushy\ phase \\ 1, & T > T_l, \quad Liquid\ phase \end{cases} \tag{6}$$

When PCM-modified asphalt concrete's temperature approaches the phase change temperature, PCM can absorb or release thermal energy heat (L). Hence, the transient heat conduction of PCM-modified asphalt concrete is expressed in Eq. (7).

$$\rho c_{p_{eff}} \frac{\partial T}{\partial t} = \frac{\partial}{\partial z}\left(k_{eff} \frac{\partial T}{\partial z}\right) - \phi \rho_{PCM} L \frac{\partial \xi}{\partial t} + Q \tag{7}$$

The MATLAB R2020a was employed to program and solve the numerical equations [27]. Fig. 2 depicts a schematic diagram of the asphalt pavement. Thermal conductivity, thickness, density, and volume fraction of PCM at the i^{th} layer were k_i, z_i, ρ_i, and ξ_i (with i = 1, 2, 3, . . ., n), respectively. The recursive numerical model was employed to analyze the transient temperature response of the PCM-modified asphalt concrete as shown in Eq. (8). Where, T_i^{p+1} and T_i^p = temperature at the time p + 1 and p (°C), respectively; Δt = time step (s); Δz = depth increment (m) ξ_i^{p+1} and ξ_i^p = PCM's fraction volume at the time p + 1 and p (%), respectively.

$$\rho c_{p_{eff}} \left(\frac{T_i^{p+1} - T_i^p}{\Delta t}\right)\Delta z = k_i\left(\frac{T_{i-1}^p - T_i^p}{\Delta z}\right) - k_i\left(\frac{T_i^p - T_{i+1}^p}{\Delta z}\right) - \phi \rho_{PCM} L \left(\frac{\xi_i^{p+1} - \xi_i^p}{\Delta t}\right)\Delta z \tag{8}$$

The unknown PCM's fraction volume (ξ^{t+1}) at the time t^{p+1} was determined by an iterative method. As shown in Eq. (9), the intermediate temperature (T_i^{m+1}) was calculated based on the temperature of the previous time (t^p). The T_i^{m+1} is then used to update the unknown ξ^{t+1}. The iterative process was repeated until $\left|\left|T^{m+1} - T^p\right|\right| < 10^{-5}$ [28].

$$\rho c_{p_{eff}}\left(\frac{T_i^{m+1}-T_i^p}{\Delta t}\right)\Delta z = k_i\left(\frac{T_{i-1}^p-T_i^p}{\Delta z}\right) - k_i\left(\frac{T_i^p-T_{i+1}^p}{\Delta z}\right) - \phi\rho_{PCM}L\left(\frac{\xi_i^{m+1}-\xi_i^p}{\Delta t}\right)\Delta z,\ m=1,2,3,\ldots \quad (9)$$

Overall, the interaction between the pavement surface and its surrounding is written in Eq. (10).

$$\rho c_{p_{eff}}\left(\frac{T_i^{p+1}-T_i^p}{\Delta t}\right)\Delta z = k_i\left(\frac{T_{i-1}^p-T_i^p}{\Delta z}\right) - k_i\left(\frac{T_i^p-T_{i+1}^p}{\Delta z}\right) - \phi\rho_{PCM}L\left(\frac{\xi_i^{p+1}-\xi_i^p}{\Delta t}\right)\Delta z + Q \quad (10)$$

This study aims to evaluate the effect of μPCM on rheological properties of asphalt binder; therefore, the PCM content is determined by the weight of asphalt binder through equation (11). Where, p_{PCM} = PCM content (%), ϕ = optimum PCM volume (%), ρ_{PCM} = PCM density (kg/m^3), p_b = binder content in asphalt mixture (%), and ρ_b = binder density (kg/m^3).

$$p_{PCM} = \frac{\phi \times \rho_{PCM}}{p_b \times \rho_b} \quad (11)$$

The temperature of PCM-modified asphalt concrete was analyzed to predict PCM's optimum contents in asphalt mixture. In this research, boundary conditions (air temperature, wind speed, and solar radiation) were obtained from South Korea's climate data, as shown in Fig. 3a [29]. The thickness of PCM-AC, base course, and subgrade was 10 cm, 15.2 cm, and 20 cm, respectively. Based on previous studies, the materials' thermophysical properties are presented in Table 1 and Table 2 [4,17,24,30]. The results from Fig. 3b shows that the PCM addition of 1.5% by wt. of asphalt mixture (7.5% by wt. asphalt binder) helps pavement temperature gain 1.5 °C higher than that of without PCM. Therefore, 2.5% and 7.5% by weight of the binder were chosen as the main contents to examine PCM's effect on the rheological property of asphalt binder.

2.2. Preparation of micro-encapsulation phase change material

2.2.1. Raw materials

In this study, n-Tetradecane ($C_{14}H_{30}$) was used as a core. The n-Tetradecane had a molecular weight of 198.39 g/mol, latent heat capacity of 154.7 J/g, and melting point of 10 °C. Two surfactants were used in this experiment. First, Tween 80 ($C_{64}H_{124}O_{26}$) had molecular weight of 1310 g/mol. Second, Span 80 ($C_{24}H_{44}O_6$) had a molecular weight of 428.6 g/mol. Shell material used in this study included calcium chloride ($CaCl_2$) and sodium carbonate (Na_2CO_3), Tetra-ethyl silicate (TEOS), Poly Vinyl Alcohol (PVA), Ethanol, and Acetic acid.

2.2.2. Preparation of μPCMs

The $CaCO_3$ micro-encapsulation process is depicted in Fig. 4. The core–shell ratio was 1:1. Firstly, the core material (n-Tetradecane) and the surfactants (Tween 80 and Span 80) were dissolved in deionized water in a 500 ml flask. The dissolved process took for 20 min with stirring speed of 300 RPM (rotation per min). Secondly, in preparation of shell material, the calcium chloride ($CaCl_2$) was dissolved in deionized water (50 ml), then dropped into the core solution, and continuously mixed for four hours at 300 RPM. The sodium carbonate solution (Na_2CO_3 + deionized water) was initiated into the mixture by dripping into the flask. After dripping, a centrifuge was employed to purify the resultant microcapsules. The process was conducted at a temperature of 35 °C. Finally, micro-encapsulation PCM was dried at 60 °C for 12 h.

The SiO_2 micro-encapsulation process is shown in Fig. 5. In this process, the core–shell ratio was the same with 1:1. The n-Tetradecane was first dissolved with an emulsifier solution of Tween 80 and Span 80. At the same time, a PVA solution was prepared by mixing deionized water and PVA in a 500 ml flask. Two solutions (core-solution and PVA-solution) were then mixed. Afterward, the TEOS and acetic acid solution were dripped into solution at 35 °C with a speed of 300 RPM for 3 h. Finally, the resulting products were filtered and washed by ethanol three times before drying in the oven at 35 °C for 24 h.

3. Test methods

3.1. Properties of micro-encapsulation phase change materials

3.1.1. Scanning electron microscope (SEM test)

The scanning electron microscope (HITACHI SU3800) was employed to observe the morphology, size, and particle shape of micro-encapsulation phase change material (Fig. 6a).

3.1.2. Thermogravimetric analysis (TGA test)

Thermogravimetric analysis is adopted to determine a material's thermal stability and fraction by monitoring the weight change [31]. In the current research, the thermal stability of different PCMs was analyzed by TA Instruments SDT Q600 (Fig. 6b). The size of a single PCM sample ranged from 1 to 5 mg. Each sample was heated from room temperature (25 °C) to 350 °C with a heating ramp of 20 °C /min under a nitrogen atmosphere. Concurrently, the weight of the sample was recorded during the whole analysis period.

3.1.3. Differential scanning calorimetry (DSC test)

Differential scanning calorimetry (DSC) measures samples' energy transfer undergoing a physical or chemical change [32]. The TA DSC250 was assigned to investigate the thermal transition of synthesized PCM (Fig. 6c). A prepared sample of 10–15 mg is shown in Fig. 6d. For each sample, the DSC test consisted of a heating and cooling process. Firstly, the sample cooled down from room temperature to −40 °C and was maintained for 5 mins. The sample was then heated to 40 °C and kept for 5 mins before cooling again to −40 °C. The test was conducted with a heating/cooling rate of 10 °C /min. The PCM's heat flow (W/g) was recorded during the process. The encapsulation ratio (R_E) was estimated to determine the effect of the encapsulation method on energy storage of μPCM. The R_E (%) was defined as the enthalpy (ΔH) ratio of μPCM by n-Tetradecane, as shown in Eq. (12).

$$R_E = \frac{\Delta H_{\mu PCM}}{\Delta H_{Tetradencan}} \times 100 \quad (12)$$

3.2. Rheological property of μPCM modified asphalt binder

3.2.1. Rotational viscosity test (RV test)

The RV test determines the viscosity of asphalt binders in the high temperature of production and construction. The smaller viscosity value at the high temperature (e.g., 135 °C) indicates the better workability of asphalt mixture in the mixing and compaction process [33]. According to Superpave binder specification, the viscosity shall not exceed 3 Pa.s [1]. In this study, the Brooked viscometer was employed to measure the viscosity of μPCM modified asphalt binder. The base binder (PG 64–22) was modified with the highest μPCM content (7.5% by weight of binder). The rotational test was conducted with a constant rotational speed of 20 RPM at 135 °C. For each replicate, the viscosity was measured at 1-min intervals for a total of 3 min [34].

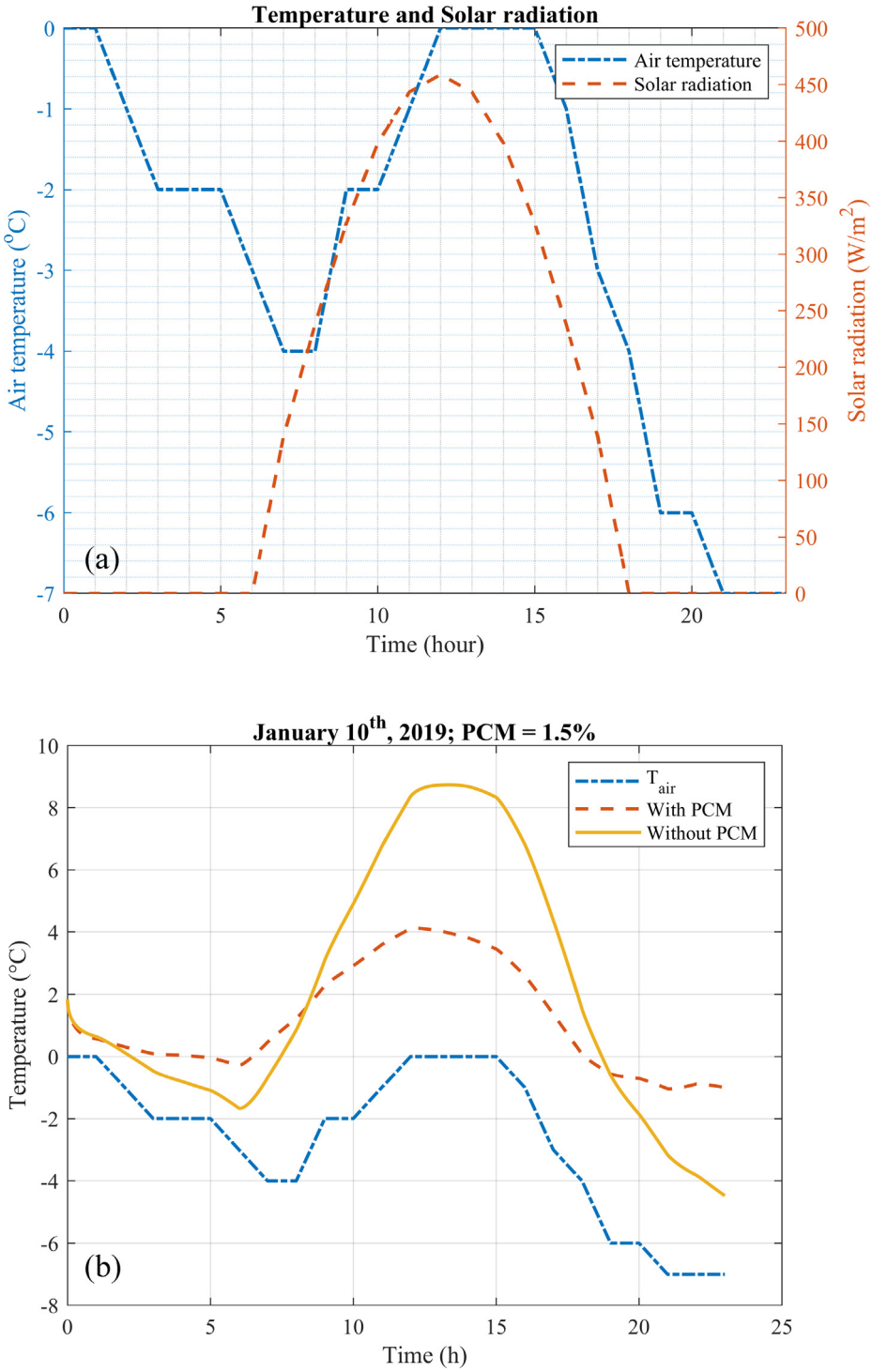

Fig. 3. (a) Climate data, (b) surface temperature of PCM-modified asphalt pavement.

Table 1
Thermophysical properties of materials.

	Thickness (cm)	Density (kg/m³)	Thermal conductivity (W/mK)	Heat capacity (J/kgK)
AC	10.2	2288	1.2	950
Base course	15.2	1950	1.0	1000
Subgrade	20.0	1760	1.0	1100

Table 2
Thermophysical properties of μPCM.

	Latent heat fusion (J/g)	Density (kg/m^3)	Thermal conductivity (W/mK)	Heat capacity (J/kgK)
T_l = 3 °C T_s = −8 °C	50	768	Liquid phase: 0.15 Solid phase: 0.37	Liquid phase: 2330 Solid phase: 1930

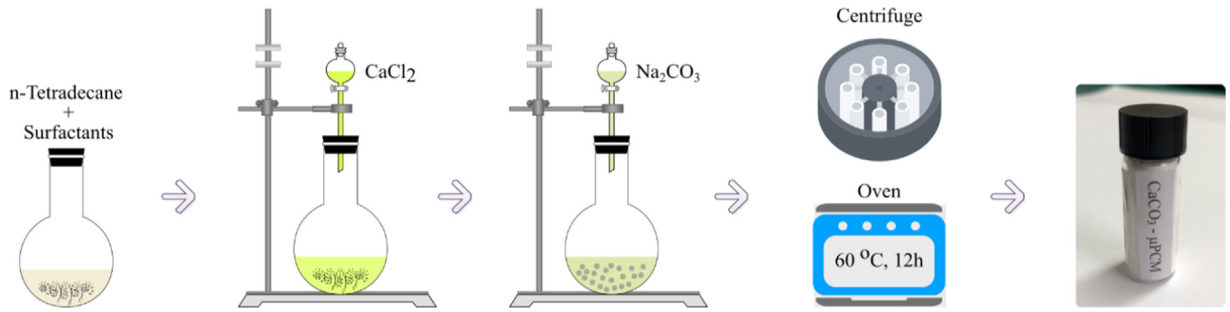

Fig. 4. The micro-encapsulation process of $CaCO_3$-μPCM.

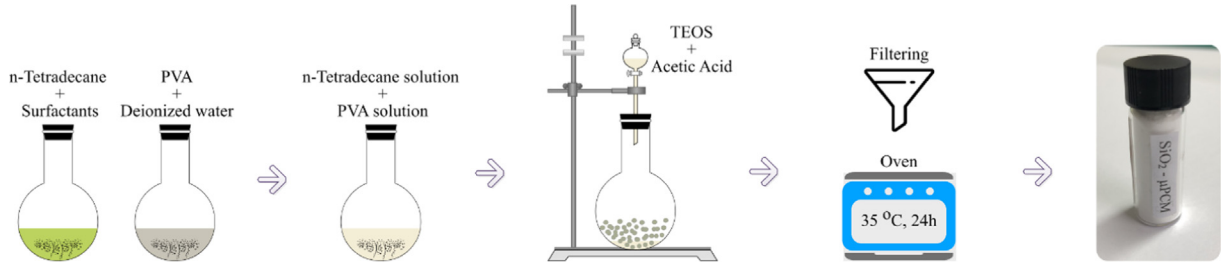

Fig. 5. The micro-encapsulation process of SiO_2-μPCM.

3.2.2. Dynamic shear rheometer (DSR test)

The dynamic shear rheometer (DSR) test was executed to measure rheological properties such as complex modulus (G^*) and phase angle (φ) parameters. Two μPCM contents were considered, including 2.5% and 7.5% by weight of binder. The DSR was examined in several temperatures, including 0 °C, 10 °C, 20 °C, 30 °C, 40 °C, 50 °C, 60 °C, and 70 °C. For each temperature, the frequency ranged from 0.1 to 20 Hz. At low temperature (0 °C–30 °C), the 25 mm diameter plate, 1 mm gap, and constant strain amplitude of 0.05% were used (Fig. 7). Otherwise, the 8 mm diameter plate, 2 mm gap and constant strain amplitude of 0.1% was used at high temperature (40 °C–70 °C) [35].

At reference temperature (T_r), the complex modulus and phase angle master curve were generated using time-temperatures superposition principle [36]. The dynamic modulus master curve and phase angle master curve were expressed in equation (13) and (14), respectively [37]. The shift factor (α_T) was employed to shift complex modulus or phase angle at a certain temperature (T) to a master curve for a reference temperature. As shown in equation (15), the shift factor was calculated based on Williams-Landel-Ferry (WLF) relation [38]. Where, G_f^*, φ_f = dynamic modulus and phase angle at frequency, respectively; f = loading frequency (Hz); δ, α, λ, β, γ = fitting parameters; α_T = time–temperature shift factor; T = test temperature (°C); T_r = reference temperature (°C); C_1, C_2 = fitting parameters.

$$\log\left|G_f^*\right| = \delta + \frac{\alpha}{1 + e^{\beta+\gamma\times\log(f\times\alpha_T)}} \tag{13}$$

$$\varphi_f = -\frac{\frac{\pi}{2}\times\alpha\times\gamma\times e^{\beta+\gamma\times\log(f\times\alpha_T)}}{\left[1+\lambda\times e^{\beta+\gamma\times\log(f\times\alpha_T)}\right]^{\left(1+\frac{1}{\lambda}\right)}} \tag{14}$$

$$\log\alpha_T = -\frac{C_1\times(T-T_r)}{C_2+(T-T_r)} \tag{15}$$

In this study, the reference temperature of 20 °C was chosen to generate the master curve of both dynamic modulus and phase angle. The MATLAB® optimization toolbox was employed to determined several unknown model parameters (i.e., δ, α, λ, β, γ, C_1, and C_2) with the minimum sum of error [27,39]. The sum of error (SE) can be referenced in equation (16). Where, SE = sum of error; N = number of measured data; $G^*_{m,\,i}$, $\varphi_{m,\,i}$ = measured dynamic modulus, measured phase angle at point ith, respectively; $G^*_{p,\,i}$, $\varphi_{p,\,i}$ = predicted modulus, predicted phase angle at point ith, respectively.

$$SE = Error_{G^*} + Error_{\varphi}$$
$$SE = \sum_{i=1}^{N}\left[\left(G^*_{m,i} - G^*_{p,i}\right)^2 + \left(\varphi_{m,i} - \varphi_{p,i}\right)^2\right] \tag{16}$$

3.2.3. Low-temperature sweep test

The low-temperature sweep test was employed to measure the thermal effect of μPCM on the rheological response of the modified asphalt binders. The specimens had a size of 8 mm in diameter with 2 mm in thickness. This test was conducted with a constant strain amplitude of 0.1% and frequency of 1 Hz. The temperature

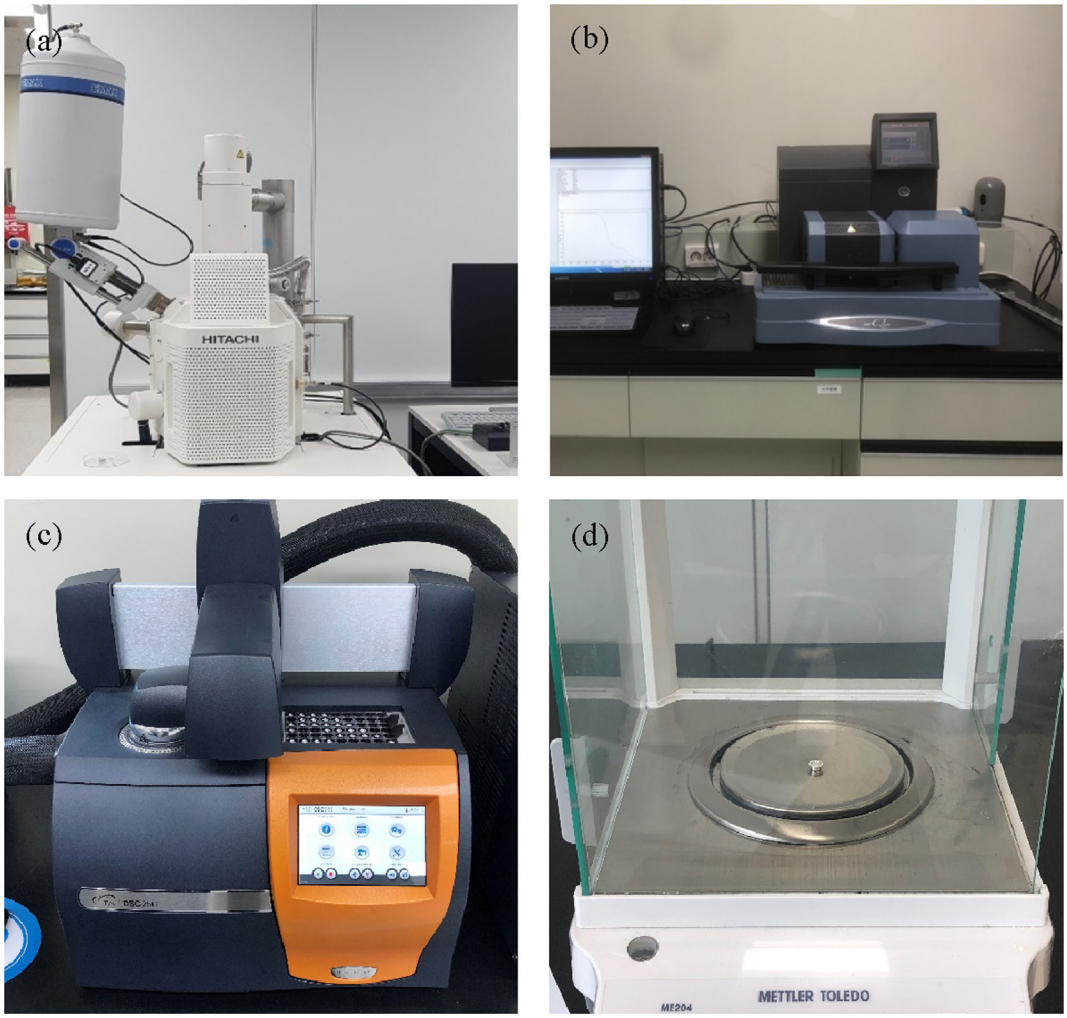

Fig. 6. (a) SEM test, (b) TGA test, and (c, d) DSC test.

was dropped from 20 °C to −10 °C with a cooling ramp of 0.44 °C / min [13].

4. Results – discussion

4.1. Micro-encapsulation PCM properties

4.1.1. Scanning electron microscope

The micro-encapsulation process can be explained through Fig. 8. Firstly, n-Tetradecane was dissolved with two surfactants. After the mixing process, the core was covered by a layer of surfactants, which formed a micelle. By adding calcium chloride ($CaCl_2$) into the n-Tetradecane-emulsion system, the Ca^{2+} was captured on a micelle surface. Then, adding sodium carbonate (Na_2CO_3) into the emulsion creates $CaCO_3$-shell. As a result, the $CaCO_3$-μPCM was synthesized with a core of n-Tetradecane and a shell of $CaCO_3$. This process was idealized based on the research of Wang et al. [18].

Fig. 9 illustrates the morphology of the two μPCMs. Overall, both μPCMs archived the perfect spherical micro-encapsulation structure as shown in Fig. 9b and Fig. 9e. The $CaCO_3$-μPCM's diameter ranged from 5 to 7 μm. The surface of $CaCO_3$-μPCM was generally quite rough as depicted in Fig. 9c. This is because of the crystalline polymorphs of $CaCO_3$. At 35 °C reaction temperature, most of $CaCO_3$ morphological structures were calcite and vaterite [40]. The small partial sizes and de-agglomeration may help μPCM easily distribute in an asphalt mixture. Meanwhile, SiO_2-μPCM showed a smaller diameter than $CaCO_3$-μPCM, which was approximately 0.9–1.5 μm (Fig. 9d). The surface of SiO_2-μPCM was generally smoother than that of $CaCO_3$-μPCM.

4.1.2. Thermogravimetric analysis

Fig. 10 depicts the thermal stability of μPCMs and core material (n-Tetradecane). This test was measured thermal stability of μPCMs under the high mixing temperature (e.g., 160 °C). Overall, the encapsulation method improved thermal stability of μPCMs. The remaining weight of the SiO_2 sample decreased to 71% at the temperature of 160 °C. Meanwhiles, the $CaCO_3$-μPCM acquired better thermal stability than that of SiO_2-μPCM. The residual weight of the $CaCO_3$ sample was reduced by 5% only at 160 °C, and slightly decreased to 84% at 350 °C. The outperformed residual weight confirmed that the $CaCO_3$-shell could reduce leakage of the core material. Therefore, the $CaCO_3$ shell is considered as an effective method for improving the thermal stability of μPCM in an asphalt mixture. As shown in Fig. 10, the n-Tetradecane exhibited a weight loss of 70% at 160 °C. However, using encapsulation methods help n-Tetradecane substantially reduce its weight loss, which was 5% and 30%, corresponding to $CaCO_3$ and SiO_2 shell, respectively. Thus, it can be concluded that both encapsulation methods showed good protection on n-Tetradecane core.

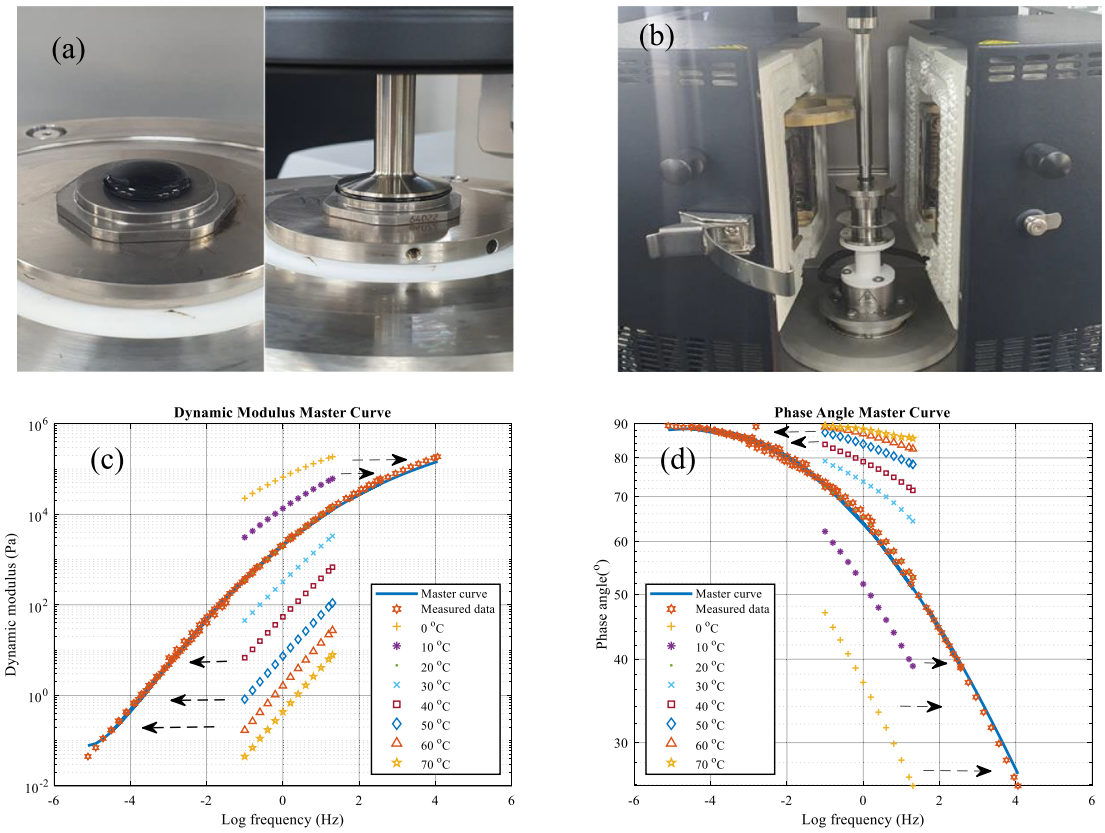

Fig. 7. (a, b) DSR test, (c) dynamic modulus, and (d) phase angle master curve generalized by WLF model.

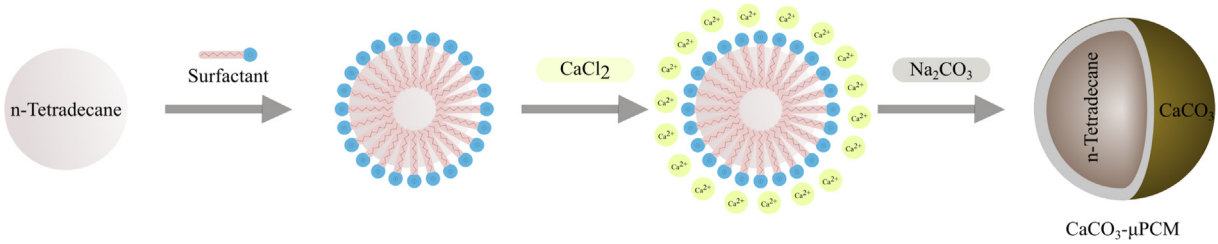

Fig. 8. $CaCO_3$-μPCM synthesis process.

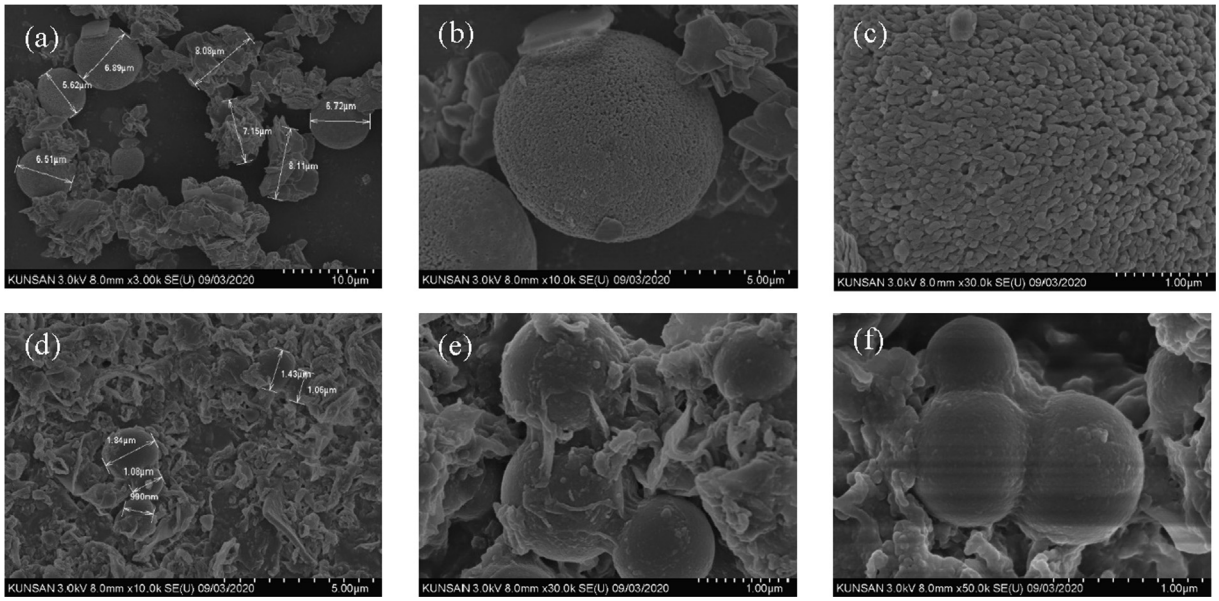

Fig. 9. Microstructure of (a, b, c) $CaCO_3$-μPCM and (d, e, f) SiO_2-μPCM.

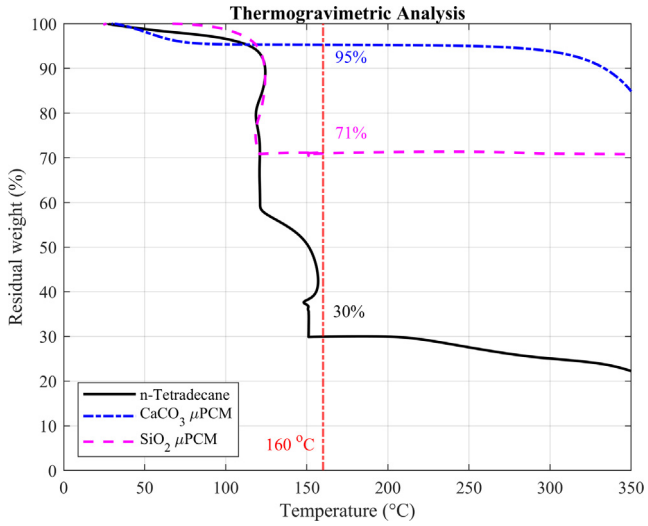

Fig. 10. Thermogravimetric analysis result.

4.1.3. Differential scanning calorimetry

The phase change properties of two μPCMs are shown in Fig. 11. The phase change temperature ranged from 0 to 6 °C, which can prevent/delay the pavement's freezing of black ice [12]. When the environment temperature approaches 0 °C (black ice occurrence), μPCM releases latent heat energy to warm the surrounding environment (asphalt mixture). The utilization of this latent heat can be used to delay the black ice formation and improve thermal cracking resistance of asphalt binder at low temperatures. The energy storage of μPCM was mainly related to the core material that releases/absorbs thermal energy. Therefore, the encapsulation (R_E) ratio indicated the storage effect of the encapsulation method. The higher R_E corresponds to better thermal energy storage. The latent heat fusion of SiO_2-μPCM was higher than that of $CaCO_3$-μPCM. The SiO_2 sample's enthalpy was approximately 99.94 J/g (R_E = 52.9%), while $CaCO_3$ presented an enthalpy of 71.83 J/g (RE = 37.9%). This can be explained by the thermal stability of $CaCO_3$-shell compared that of SiO_2-shell (as mentioned in 4.1.2), which may reduce the release latent heat of core material. Moreover, the difference of melting and freezing point between n-Tetradecane and μPCMs indicated that the shell material slightly delayed the phase change process.

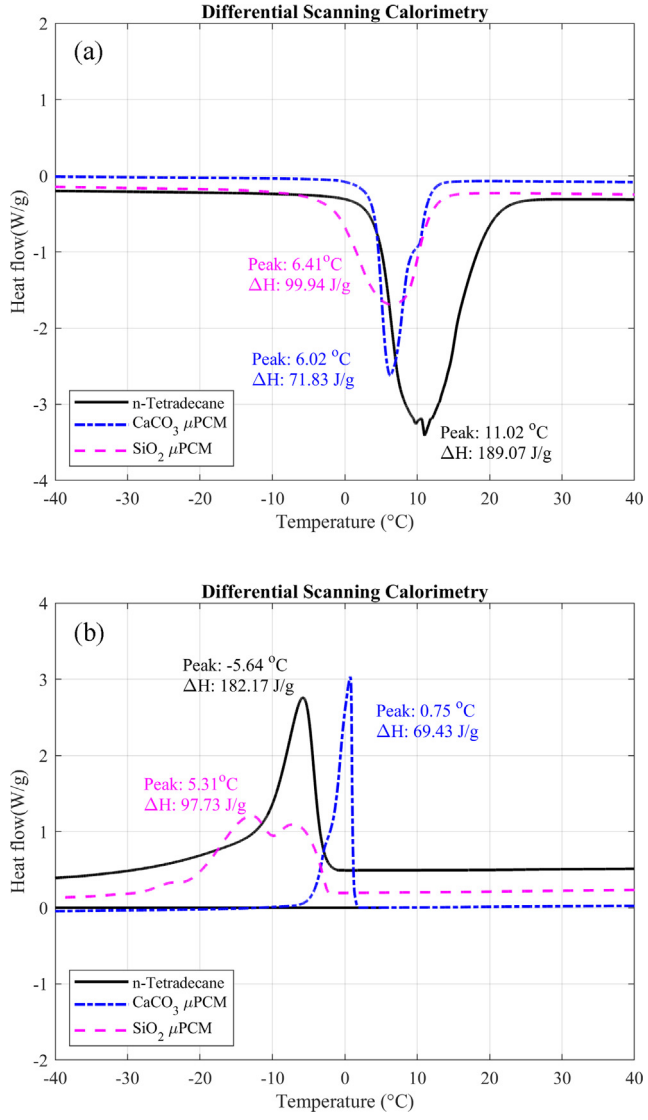

Fig. 11. DSC curves of $CaCO_3$ and SiO_2 μPCM: (a) cooling curve, (b) heating curve.

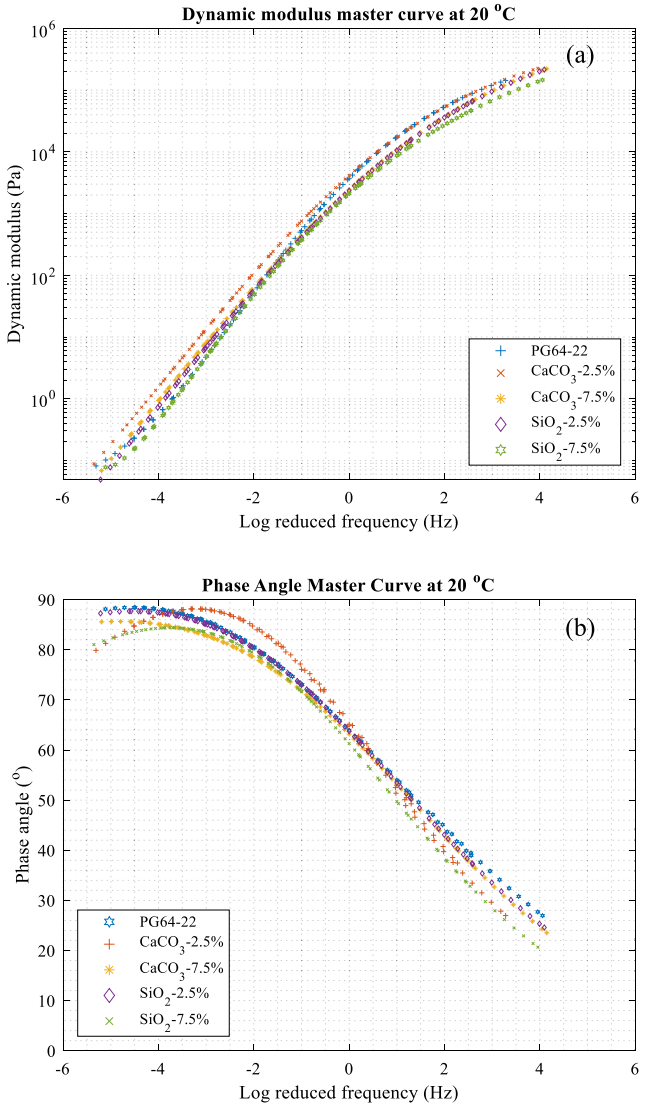

Fig. 12. (a) Dynamic modulus and (b) phase angle master curves of μPCM modified asphalt binders.

Table 3
Parameters of master curves model.

Mix types	δ	α	λ	β	γ	C_1	C_2	SE
PG 64–22	11.59	7.40	0.18	−0.99	−0.42	36.67	191.26	1.12
$CaCO_3$-μPCM-2.5%	14.15	20.19	4.61	−1.75	−0.39	17.44	146.55	1.26
$CaCO_3$-μPCM-7.5%	13.79	19.13	3.86	−1.41	−0.43	13.58	115.06	1.15
SiO_2-μPCM-2.5%	7.53	13.89	1.36	−1.75	−0.39	17.14	123.15	1.13
SiO_2-μPCM-7.5%	6.00	12.51	0.71	−1.11	−0.29	15.46	134.04	1.21

4.2. Rheological properties

4.2.1. Rotational viscosity

Among the different contents, the highest μPCM dosage (7.5% by wt.) was chosen to analyze rotational viscosity behavior. The rotational viscosity of 7.5% μPCM modified asphalt binder was approximately 0.5 Pa.s at the temperature of 135 °C. Based on the Superpave specification of asphalt binder, the RV has met the criterion of 3 Pa.s [1]. It could be found that the addition of μPCM did not affect viscosity of asphalt binder at the high range temperature. In other words, the addition of μPCM did not affect the production and compaction of asphalt mixture.

4.2.2. Dynamic shear rheometer

The dynamic modulus master curves are illustrated in Fig. 12a. In this study, the reference temperature was 20 °C. For each μPCM, two different contents were examined (e.g., 2.5% and 7.5%). The predicted parameters are shown in Table 3. Overall, asphalt binder containing μPCM obtained a lower dynamic modulus at low temperatures or high frequencies compared to the control one. The SiO_2-μPCM-7.5% presented the lowest dynamic modulus value at high frequencies (low temperatures). This can be explained that the latent heat released by the addition of μPCM which help warming the surrounded binder and thereby, mitigating the increase in binder stiffness. In other words, μPCM could improve the thermal cracking resistance of asphalt binder. When temperature increases, the $CaCO_3$-μPCM-7.5% gained the highest dynamic modulus, improving rutting resistance. At this stage, the effect of latent heat was negligible; thereby, μPCMs played a role as mineral particles. Fig. 12b illustrates phase angle master curves of μPCM modified asphalt binders. The phase angle is an indicator which demonstrates the ratio of viscosity and elasticity. The μPCM modified asphalt binders obtained a lower phase angle than the base binder at the high frequencies or low temperatures. The lower phase angle indicated less viscous behavior. Therefore, the asphalt binder can deter the occurrence of low temperature cracking.

Fig. 13 shows dynamic modulus and phase angle at different frequencies (e.g., 0.1 Hz, 1.0 Hz, 10 Hz, and 20 Hz). Overall, the dynamic modulus decreased while the phase angle increased when the temperature was elevated. At the low temperature (0–10 °C),

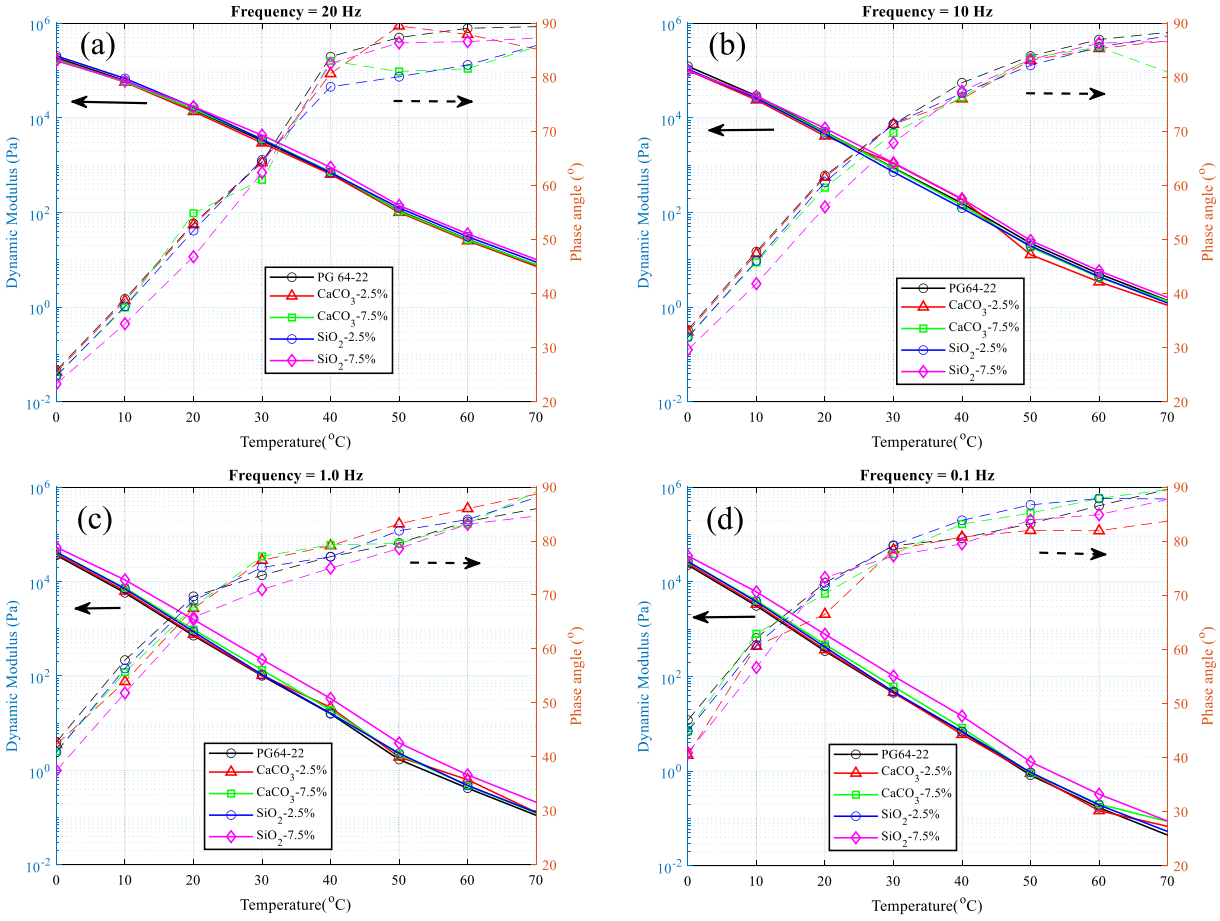

Fig. 13. Dynamic modulus and phase angle at different frequencies.

asphalt binders presented viscous behavior; however, μPCM modified asphalt binders exhibited a lower dynamic modulus than PG 64–22 binder. Especially, the SiO_2-μPCM-7.5% modified binder acquired the lowest dynamic modulus value. It can be explained by the latent heat effect from the μPCM, which reduced the stiffness of the asphalt binder as mentioned before. At the high range temperature (60–70 °C) and low frequencies (e.g., 0.1 Hz and 1.0 Hz), binders containing μPCM gained a higher dynamic modulus value than the unmodified binder. This phenomenon may be due to the phase transition of μPCMs has undergone at the low temperature (phase change temperature range of 0–6 °C). Thereby, the effect of latent heat was negligible at high temperature range. When the influence of latent heat was insignificant the μPCM acts as the mineral component, which could contribute to the stiffness reinforcement of asphalt binder [22].

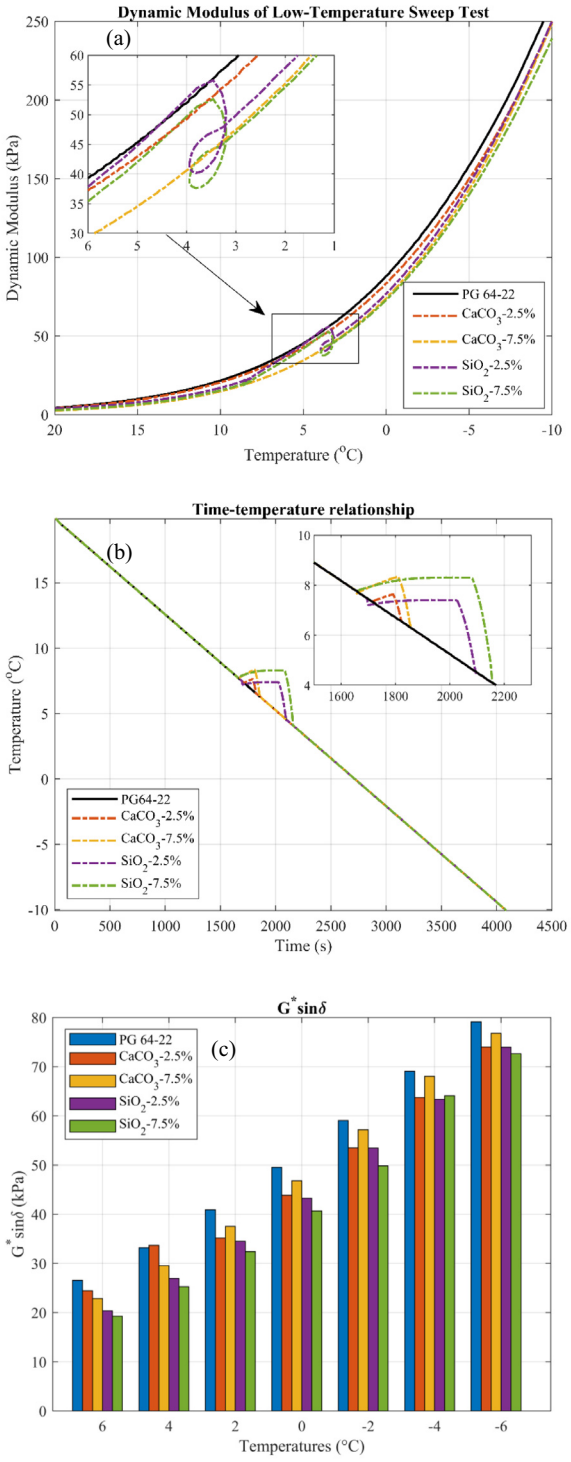

Fig. 14. (a) Dynamic modulus and (b) time–temperature relationship, and (c) G*sinδ.

4.2.3. Low-temperature sweep test

The low-temperature sweep test examined the thermal effect of μPCM on the rheological property of modified asphalt binders. Dynamic modulus and phase angle of modified binders were recorded during the cooling process (from 20 °C to −10 °C). The results infer that asphalt binders containing μPCM obtained a lower dynamic modulus than the base one. Generally, the dynamic modulus values increased when the temperature decreased. Moreover, both μPCMs gained a lower dynamic modulus value than that of an un-modified asphalt binder. The SiO_2 samples presented discontinuous curves during phase change temperature, as shown in Fig. 14a. When the environment temperature dropped to 4 °C, the dynamic modulus value suddenly decreased by 55 to 40 kPa. At the same time, μPCM released the latent heat, which increased the whole sample's temperature by 1.5 °C. Then, the dynamic modulus value of μPCM modified asphalt mixture continuously increased. However, it was found that the temperature of modified mixture still maintains lower than the base asphalt binder (PG 64–22). It can be concluded that asphalt binder containing μPCM could reduce stiffness at the low temperature.

The temperature involved time of PCM modified asphalt binders is displayed in Fig. 14b. As expected, μPCM modified asphalt binder gained a higher temperature than the control sample due to the release of latent heat. However, the temperature difference of $CaCO_3$-μPCM was insignificant compared to that of SiO_2-μPCM. This may be due to the latent heat capacity, as proved in the 4.1.3 section. The discontinuous curves were only recorded in SiO_2-μPCM samples. Meanwhiles, the $CaCO_3$-PCM with small latent heat capacity (approximately 70 J/g) and larger size (5–7 μm) presented continuous curves, as shown in Fig. 14a.

Moreover, the sample binder temperature increased at the phase transition of μPCM, the G*sinδ values were calculated at variable temperatures such as 6, 4, 2, 0, −2, −4, and −6 °C to verify the effect of μPCM on low temperature cracking (Fig. 14c). Based on the study of Brown et al., the lower G*sinδ value indicated a better low temperature cracking resistance [1]. This behavior was observed for SiO_2-μPCM-7.5%, gaining the lowest value among different asphalt binders. Meanwhile, the conventional asphalt binder showed the highest G*sinδ value. Overall, the addition of both types and mixture weight percentage of μPCM could improve the thermal cracking resistance of asphalt binder at low temperature.

5. Conclusions

In this study, two micro-encapsulation phase change materials (μPCMs) are synthesized for heat energy storage, including $CaCO_3$-μPCM and SiO_2-μPCM. The improvement on rheological properties of μPCM modified asphalt binder were confirmed by the dynamic shear rheometer test and the low-temperature sweep test. The following key findings can be drawn:

- Two micro-encapsulation phase change materials were successfully synthesized with the core–shell ratio of 1:1. Both μPCMs archived the perfect spherical micro-encapsulation structure. The diameter of $CaCO_3$-μPCM and SiO_2-μPCM ranged from 5 to 7 μm and 0.9–1.5 μm, respectively.

- The SiO_2-μPCM acquired a higher latent heat of 99.94 J/g (R_E = 52.9%) compared to that of $CaCO_3$-μPCM, which was 71.83 J/g (R_E = 37.9%). However, the $CaCO_3$-PCM presented better thermal stability than SiO_2-μPCM at high temperature (160 °C).
- Due to the micro-size of μPCM, containing 7.5% μPCM did not affect the rotational viscosity of asphalt binder at high temperature (135 °C).
- At low temperature, the incorporation of μPCMs could reduce the stiffness of asphalt binder. The calculated $G^*\sin\delta$ values of μPCMs modified asphalt binder were lower than that of conventional asphalt binder. In other words, the utilization of appropriate μPCM could improve the low temperature cracking resistance.
- The low-temperature sweep test results showed that the dynamic modulus of modified binders strongly decreased during phase transition. Due to the release of latent heat, the temperature of the whole asphalt binder sample was increased by 1.5 °C, which is significantly beneficial in mitigating black ice formation.

In general, this study provides a method to synthesize μPCMs for heat energy storage. The thermal stability and latent heat storage of μPCM were acceptable. The addition of μPCM could enhance the low temperature cracking resistance of asphalt binder. It should be noted that more analysis on the effect μPCMs on asphalt mixture should be considered in further research.

CRediT authorship contribution statement

Tam Minh Phan: Methodology, Software, Validation, Data curation, Writing - original draft, Writing - review & editing. **Dae-Wook Park:** Conceptualization, Methodology, Validation, Data curation, Writing - review & editing. **Tri Ho Minh Le:** Validation, Data curation, Writing - original draft, Writing - review & editing.

Declaration of Competing Interest

The authors declare that they have no known competing financial interests or personal relationships that could have appeared to influence the work reported in this paper.

Acknowledgements

This research was supported by a grant from Infrastructure and Transportation Technology Promotion Research Program funded by the Ministry of Land, Infrastructure and Transport of Korean Government (Code **20CTAP-C157548-01**).

References

[1] T.W.K. E. Ray Brown, Prithvi S. Kandhal, Freddy L. Roberts, Y. Richard Kim, Dah-Yinn Lee, Hot mix asphalt materials, mixture design, and construction, 2009.
[2] M. Southern, A perspective of bituminous binder specifications, in: S.-C. Huang, H.B.T.-A. in A.M. Di Benedetto (Eds.), Woodhead Publ. Ser. Civ. Struct. Eng., Woodhead Publishing, Oxford, 2015: pp. 1–27. 10.1016/B978-0-08-100269-8.00001-5.
[3] Å. Hermansson, Mathematical model for calculation of pavement temperatures: comparison of calculated and measured temperatures, Transp. Res. Rec. 1764 (1) (2001) 180–188, https://doi.org/10.3141/1764-19.
[4] M.R. Hall, P.K. Dehdezi, A.R. Dawson, J. Grenfell, R. Isola, Influence of the thermophysical properties of pavement materials on the evolution of temperature depth profiles in different climatic regions, J. Mater. Civ. Eng. 24 (1) (2012) 32–47, https://doi.org/10.1061/(ASCE)MT.1943-5533.0000357.
[5] J.J. Stempihar, T. Pourshams-Manzouri, K.E. Kaloush, M.C. Rodezno, Porous asphalt pavement temperature effects for urban heat island analysis, Transp. Res. Rec. 2293 (1) (2012) 123–130, https://doi.org/10.3141/2293-15.
[6] K.T. Nguyen, Q.D. Nguyen, T.A. Le, J. Shin, K. Lee, Analyzing the compressive strength of green fly ash based geopolymer concrete using experiment and machine learning approaches, Constr. Build. Mater. 247 (2020), https://doi.org/10.1016/j.conbuildmat.2020.118581 118581.
[7] T.M. Phan, D.-W. Park, T.H.M. Le, Crack healing performance of hot mix asphalt containing steel slag by microwaves heating, Constr. Build. Mater. 180 (2018) 503–511, https://doi.org/10.1016/j.conbuildmat.2018.05.278.
[8] T.M. Phan, S.N. Nguyen, C.-B. Seo, D.-W. Park, Effect of treated fibers on performance of asphalt mixture, Constr. Build. Mater. 274 (2021), https://doi.org/10.1016/j.conbuildmat.2020.122051 122051.
[9] K.V.A. Pham, T.K. Nguyen, T.A. Le, S.W. Han, G. Lee, K. Lee, Assessment of performance of fiber reinforced geopolymer composites by experiment and simulation analysis, Appl. Sci. 9 (16) (2019) 3424, https://doi.org/10.3390/app9163424.
[10] T.M. Phan, T.H.M. Le, D.-W. Park, Evaluation of cracking resistance of healed warm mix asphalt based on air-void and binder content, Road Mater. Pavement Des. (2020), https://doi.org/10.1080/14680629.2020.1829010.
[11] J. Norambuena-Contreras, A. Garcia, Self-healing of asphalt mixture by microwave and induction heating, Mater. Des. 106 (2016) 404–414, https://doi.org/10.1016/j.matdes.2016.05.095.
[12] B.J. Manning, P.R. Bender, S.A. Cote, R.A. Lewis, A.R. Sakulich, R.B. Mallick, Assessing the feasibility of incorporating phase change material in hot mix asphalt, Sustain. Cities Soc. 19 (2015) 11–16, https://doi.org/10.1016/j.scs.2015.06.005.
[13] M.R. Kakar, Z. Refaa, J. Worlitschek, A. Stamatiou, M.N. Partl, M. Bueno, Effects of aging on asphalt binders modified with microencapsulated phase change material, Compos. Part B Eng. 173 (2019), https://doi.org/10.1016/j.compositesb.2019.107007 107007.
[14] Y. Chen, H. Wang, Z. You, N. Hossiney, Application of phase change material in asphalt mixture – a review, Constr. Build. Mater. 263 (2020), https://doi.org/10.1016/j.conbuildmat.2020.120219 120219.
[15] L.H. He, J.R. Li, H.Z. Zhu, Analysis on application prospect of shape-stabilized phase change materials in asphalt pavement, Appl. Mech. Mater. 357–360 (2013) 1277–1281, https://doi.org/10.4028/www.scientific.net/AMM.357-360.1277.
[16] M.Z. Chen, J. Hong, S.P. Wu, W. Lu, G.J. Xu, Optimization of Phase Change Materials Used in Asphalt Pavement to Prevent Rutting, in: Adv. Res. Inf. Sci. Autom. Mater. Syst., Trans Tech Publications Ltd, 2011: pp. 1375–1378. https://doi.org/10.4028/www.scientific.net/AMR.219-220.1375.
[17] Z. Refaa, M.R. Kakar, A. Stamatiou, J. Worlitschek, M.N. Partl, M. Bueno, Numerical study on the effect of phase change materials on heat transfer in asphalt concrete, Int. J. Therm. Sci. 133 (2018) 140–150, https://doi.org/10.1016/j.ijthermalsci.2018.07.014.
[18] T. Wang, S. Wang, R. Luo, C. Zhu, T. Akiyama, Z. Zhang, Microencapsulation of phase change materials with binary cores and calcium carbonate shell for thermal energy storage, Appl. Energy. 171 (2016) 113–119, https://doi.org/10.1016/j.apenergy.2016.03.037.
[19] Y. Fang, H. Wei, X. Liang, S. Wang, X. Liu, X. Gao, Z. Zhang, Preparation and thermal performance of silica/n-tetradecane microencapsulated phase change material for cold energy storage, Energy Fuels 30 (11) (2016) 9652–9657, https://doi.org/10.1021/acs.energyfuels.6b01799.
[20] Z. Sun, J. Yi, Y. Huang, D. Feng, C. Guo, Properties of asphalt binder modified by bio-oil derived from waste cooking oil, Constr. Build. Mater. 102 (2016) 496–504, https://doi.org/10.1016/j.conbuildmat.2015.10.173.
[21] G. Hao, Y. Wang, K. Zhao, W. Huang, Property changes of SBS modified asphalt binders during short-term aging and implications on quality management, Constr. Build. Mater. 244 (2020), https://doi.org/10.1016/j.conbuildmat.2020.118323 118323.
[22] M. Bueno, M.R. Kakar, Z. Refaa, J. Worlitschek, A. Stamatiou, M.N. Partl, Modification of asphalt mixtures for cold regions using microencapsulated phase change materials, Sci. Rep. 9 (2019) 20342, https://doi.org/10.1038/s41598-019-56808-x.
[23] A. Hassn, M. Aboufoul, Y. Wu, A. Dawson, A. Garcia, Effect of air voids content on thermal properties of asphalt mixtures, Constr. Build. Mater. 115 (2016) 327–335, https://doi.org/10.1016/j.conbuildmat.2016.03.106.
[24] H.E. Saad, K.S. Kaddah, A.A. Sliem, A. Rafat, M.A. Hewhy, The effect of the environmental parameters on the performance of asphalt solar collector, Ain Shams Eng. J. 10 (4) (2019) 791–800, https://doi.org/10.1016/j.asej.2019.04.005.
[25] S. Mousavi Maleki, H. Hizam, C. Gomes, Estimation of hourly, daily and monthly global solar radiation on inclined surfaces: models re-visited, Energies. 10 (1) (2017) 134, https://doi.org/10.3390/en10010134.
[26] T.S.W. Karol Pietrak, A review of models for effective thermal conductivity of composite materials, J. Power Technol. 95 (2015).
[27] MathWorks, Matlab R2020a, (2020).
[28] T. Kousksou, A. Jamil, Y. Zeraouli, J.-P. Dumas, DSC study and computer modelling of the melting process in ice slurry, Thermochim. Acta. 448 (2) (2006) 123–129, https://doi.org/10.1016/j.tca.2006.07.004.
[29] Korea Meterological Administration, (n.d.). https://www.kma.go.kr/.
[30] M.T. Phan, D.-W. Park, H.-S. Kim, Simulation on heat transfer of phase change material modified asphalt concrete for delaying black ice formation, Int. J. Highw. Eng. 22 (202AD) 35–43. https://doi.org/doi.org/10.7855/IJHE.2020.22.6.035.
[31] S. Thomas, R. Thomas, A.K. Zachariah, R.K.B.T.-T. and R.M.T. for N.C. Mishra, eds., Thermal and Rheological Measurement Techniques for Nanomaterials Characterization, in: Micro Nano Technol., Elsevier, 2017: p. iv. 10.1016/B978-0-323-46139-9.12001-8.

[32] D.H.-J.F. Dr. G. W. H. Höhne, Dr. W. F. Hemminger, Differential Scanning Calorimetry, 2003.
[33] Liqun Zhang, Michael L. Greenfield, Relaxation time, diffusion, and viscosity analysis of model asphalt systems using molecular simulation, J. Chem. Phys. 127 (19) (2007) 194502, https://doi.org/10.1063/1.2799189.
[34] AASHTO-T316-13, Viscosity Determination of Asphalt Binder Using Rotational Viscometer, 2013.
[35] EN 14770, Bitumen and bituminous binders–Determination of complex shear modulus and phase angle–Dynamic Shear Rheometer (DSR), 2012.
[36] P.T. K., W.M. W., B.R. F., Asphalt Mix Master Curve Construction Using Sigmoidal Fitting Function with Non-Linear Least Squares Optimization, Recent Adv. Mater. Charact. Model. Pavement Syst. (2020) 83–101. 10.1061/40709(257)6.
[37] Y. Hui, Y. Zhanping, L. Liang, G.S. Wei, D. Chris, Evaluation of the master curves for complex shear modulus for nano-modified asphalt binders, CICTP 2020 (2012) 3399–3414, https://doi.org/10.1061/9780784412442.345.
[38] M.L. Williams, R.F. Landel, J.D. Ferry, The temperature dependence of relaxation mechanisms in amorphous polymers and other glass-forming liquids, J. Am. Chem. Soc. 77 (14) (1955) 3701–3707, https://doi.org/10.1021/ja01619a008.
[39] H. Liu, R. Luo, Development of master curve models complying with linear viscoelastic theory for complex moduli of asphalt mixtures with improved accuracy, Constr. Build. Mater. 152 (2017) 259–268, https://doi.org/10.1016/j.conbuildmat.2017.06.143.
[40] K.-Y. Chong, C.-H. Chia, S. Zakaria, Polymorphs calcium carbonate on temperature reaction, AIP Conf. Proc. 1614 (2014) 52–56, https://doi.org/10.1063/1.4895169.